

Adsorption of Cadmium from Aqueous Solution by Preparation and Characterization of Copper Nanocomposites

Asmaa B. kareem¹, Noor bashar daood², and Fatima Muafaq Abd-Alhussein³
^{1,2,3}pharmacy department, Bilad Alrafidain University College, Diyala, Iraq.

Email: asumalbayaty@gmail.com

Abstract

Copper Nanocomposites were synthesized by two different methods under extremely precise conditions. After the preparation of the samples, XRD, SEM, FTIR, and AFM, were used to evaluate the samples. where XRD and FTIR results showed good agreement with peak sites with standard and SEM results gave a clear agglomeration of the material atoms and AFM gave an average diameter 21.45 nm for CuOm and 82.01 nm for CuOn. The adsorption efficiency of the sample were studied by applying a set of batch experiments for Cadmium. The results shown at 50ppm for the batch process the degree of removal for Cd was determined as (99%) while the CuOn sample was in efficient. Also, optimum pH was measured, and it found to be ranged between (5-7) and optimum weight of CuOm was found to be (0.3 g).

Keywords: Nanocomposites, batch adsorption, X-Ray Diffraction, SEM

1. Introduction

Heavy metals are scattered all over the environment as a consequence of soil wearing away, manufacturing and farming processes. The toxic effluence of heavy farming metals are due to their intrusion with the biochemistry of the body causing a variety of illnesses [1]. The most heavy metal have devastating effects on the ecological balance and the long term effects of which might not be yet known. These metals are present in the form of oxides or sulfides or as a salt of iron, sodium, calcium, copper, etc. Heavy metal exposure in humans can occur naturally, industrially, or via unexpected sources. The use of pesticides, natural mineral deposits, or improper disposal of metals and chemicals can all lead to the contamination of drinking water [2].

Nanotechnology played important role in essential inventions in atomic and molecular size material manipulation to radically change the producing agent's properties and due to their exclusive properties, nano-composite agents are commonly used in different fields. Nanotechnology functionalizes the design, building and using of useful structures with at smallest amount of one characteristic size in nanometers [3]. Due to their unique features and potential uses, nanomaterials involving transition metals and metal oxides have become one of the trendiest areas in materials science. These materials' shape and size have a significant impact on their characteristics [4]. Because of their advantages including nontoxicity, abundance, excellent optical absorptivity, and low band gap energies, supported and unsupported Copper and Copper oxide nanoparticles are among the many materials currently available that are of great interest [5].

2. Experimental

2.1 Materials

Copper sulfate $\text{Cu}(\text{SO}_4)_2 \cdot 4\text{H}_2\text{O}$ was collected from GRM630 and diammonium phosphate $(\text{NH}_4)_2\text{HPO}_4$ from Certified for ISO 9001:2008 Sodium hydroxide pellets were purchased from Scharlau, Spanish and $3\text{CdSO}_4 \cdot 8\text{H}_2\text{O}$ Cadmium Sulphate from England and Copper (II) chloride dihydrate gathered from Merck in India. Throughout the experiment, solutions and washes were prepared using distilled and deionized water.

2.2. Methods

2.2.1 Preparation of Nanocomposite Adsorbent

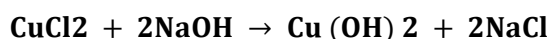
2.2.1.1 Com Nanoparticles synthesized by Microwave Enhancement

The preparation process begins with the addition of a quantity of materials copper sulfate $\text{Cu}(\text{SO}_4)_2 \cdot 4\text{H}_2\text{O}$ and the diammonium phosphate $(\text{NH}_4)_2\text{HPO}_4$ to 100 ml of distilled-water (DW) was overflowing in 250 ml glass-beaker to each constituent, the two constituents were supplementary constantly with rousing to dissolve will awaiting acquire a saturated aqueous, and then the aqueous were alienated from the residual undissolved materials in the base of glass-beaker. The inundated aqueous of $\text{Cu}(\text{SO}_4)_2 \cdot 4\text{H}_2\text{O}$ was putted in beaker and the saturated $(\text{NH}_4)_2\text{HPO}_4$ was overflowing into pipit. The preliminary of tests where gradually dropped of pipit aqueous into the glass-beaker aqueous at ambient temperature 25°C approximately, the hydrogen function (pH) of $\text{Cu}(\text{SO}_4)_2 \cdot 4\text{H}_2\text{O}$ aqueous is 11 but when $(\text{NH}_4)_2\text{HPO}_4$ aqueous was supplementary the hydrogen function of combination will fall sharply to 2, therefore NaOH aqueous was supplementary to

the combination to raise the hydrogen function to 7, then the combination was stirred by magnetic stirrer until a homogeneous aqueous is achieved, then was heated utilizing microwave emission of 800 Watt per 5 min, the precipitation was separated and lastly dehydrated at 110°C per 3 hr. Then take resulting material and analysis by XRD, FTIR, SEM, EDX, and AFM [5].

2.2.1.2 Copper Oxide Nanoparticles

CuO-NPs were synthesized according to the chemical precipitation method [3]. The method is starting by dissolving of 9000 mg CuCl₂.2H₂O and 5400 mg of NaOH tablet in CH₃CH₂OH independently. The amount of CH₃CH₂OH was as minimum amount as necessary to dissolve CuCl₂.2H₂O and NaOH independently. By using steady state mixing at ambient conditions, the addition of a suitable amount of NaOH aqueous to CuCl₂.2H₂O aqueous was revealed. The color of the aqueous solution was converted from green color to bluish-green color and lastly to black color as the chemical reaction proceed. The black impulsive was Cu (OH)₂. The impulsive was separated by using centrifuge filtration (Hettich-Germany). To remove NaCl salt aqueous, the effluent is washed with CH₃CH₂OH and de-ionized distill water. Next, the precipitate was dehydrated at 50°C using adryer. The dehydrated test sample was annealed at 600°C to obtain CuO-NPs black crystals. The annealed sample was crushed to obtain NPs powder. The chemical reaction is represented as:



Then the NPs powder was analyzed by XRD, FTIR, SEM, EDX, and AFM instruments.

2.2.2 Cadmium Sulphate Solution

A standard-stock solution was prepared at room temperature, For Cd (II) ions, a stock of aqueous solution of 1000 mg/L was made by dissolution 2282 mg of CdSO₄·8H₂O within (1 L) DI, then Different concentrations of Cadmium (II) were made by suitable dissolving of the aqueous stock-standards with appropriate capacities of DI. The pH of the solution was adjusted with 0.1 M NaOH or 0.1 M H₂SO₄.

2.3 Adsorption Batch Experiments

Adsorption experimental runs have been conceded out at ambient temperature utilizing Shaker (NHENCHPCOO5) and round bottom flasks at constant agitation speed (60 rpm). From the top made aqueous stock-solution various concentrations of cadmium (II) and combination were made by dissolving of specified capacity of the aqueous stock-solution 0.05 L of Cd (II) aqueous solution of its ions of preferred concentrations (50-125 mg/L) with various dosages of adsorbents (100-300 mg) was diverse by shaker per time intervals (15-90 min) after that the samples filtered by centrifuge, the remaining concentration of Cd(II) ions were

calculated by AAS [6]. The consequence of hydrogen function on the metal adsorption rate was attuned in range (2-12). The preliminary pH of the aqueous metal-solution was proscribed to preferred value within 10-1 mol/L NaOH or 10-1 mol/L H₂SO₄. The elimination percentage of Ni (II) and Cd (II) were calculated using the following equation: -

$$\% \text{Removal} = \frac{C_o - C_e}{C_o} \times 100 \quad 1$$

Where, C_o and C_e are the initial and final concentrations (mg/L) of Cd (II).

The adsorbed amount is then calculated using the following equation:

$$q_e = \frac{(C_o - C_e)V}{m} \times 100 \quad 2$$

Where, V is the volume of the sample, m weight of the adsorbent, C_o, C_e is the initial and equilibrium concentration respectively.

3. Result and Discussions

3.1 Morphology Analysis

3.1.1 X-Ray Diffraction Analysis (XRD)

3.1.1.1 CuO Nanoparticles Synthesized by Microwave Enhancement

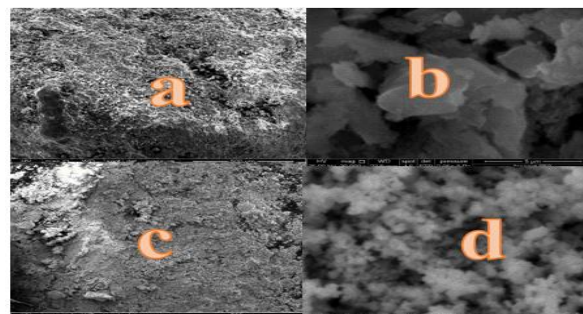


figure 1. XRD patterns of Cuom

X-ray diffraction technique was done in the University of Baghdad - Geological Science department. Data were collected within the 2θ range of 4.99° and 55° using CuKα radiation Nickel filter (λ=1.54Å). An XRD was employing a Siemens D5000. In this method, we observe a slight deviation in the peaks in the figure (1) below from the standard where the peaks appear in the range of (2θ=9°- 12°) The reason for the difference may be the use of a microwave oven for domestic, not industrial use, while the sample was highly efficient in adsorption of heavy metal [5].

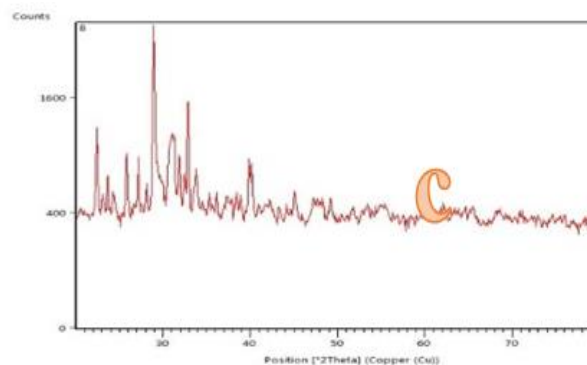


Fig 2. XRD patterns of Cuon calcinated at 600 °C for 3h

3.1.1.2 Copper Oxide Nanoparticles

As shown in Figure 2, the intensities of the peaks and peaks positions are remarkably similar to that of the illustrated values mentioned in the standard [3]. It was clearly observed that the peaks in the range of ($2\theta=35^\circ-40^\circ$), ($2\theta=48^\circ$), and ($2\theta=65^\circ-75^\circ$), which are the most important peaks exist.

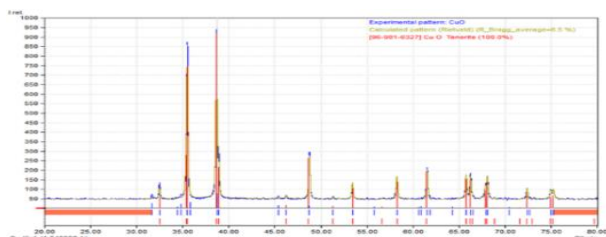


Fig 3. SEM Image at different magnification for Sample. (a), (b) CuO_m. (c), (d) CuO_n

3.1.2 Scanning Electron Microscopy & Energy Dispersive X-Ray

The morphology and the chemical composition of prepared copper Nanocomposites were investigated by SEM analysis, SEM image at different Magnification data was gathered. Figure (3) show SEM of sample CuO_m and CuO_n, these statistics show the particles growing up and crystal form happening and decant form. From these statistics, the nano-particles are agglomerate with clear morphology [7]. The nanoparticles are approximately sphere-shaped and have various radiuses. It is obvious from these statistics that Cu Nanocomposites has a normal arrangement after modification.

3.1.3 Atomic Force Microscopy (AFM)

3.1.3.1 CuO_m Nanoparticles Synthesized by Microwave Enhancement

Figure 4 (a,b) confirm that nano copper particles with the hexagonal structure were obtained. Figure 5 shows the particle size distribution of copper Nanocomposites which confirmed that of prepared CuO_m are the range of (6–100 nm) and an average diameter of 21.45 nm.

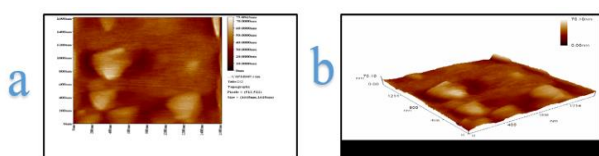


Fig 4. (a) AFM two dimensional image for Sample CuO_m (b) AFM three dimensional image for Sample CuO_m.

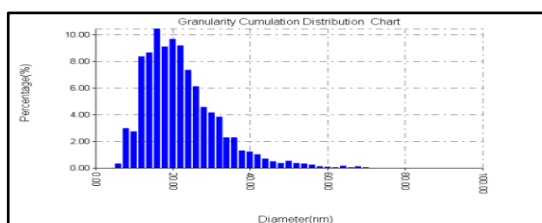


Fig 5. Granularity accumulation distribution for sample CuO_m

3.1.3.2 CuO Copper Oxide Nanoparticles

Figure 6 (a, b) confirm that nano copper particles with hexagonal structure were obtained. Figure 7 show the particle size distribution of copper Nanocomposites which confirmed that CuO_n was prepared in the range of (30–510 nm) and an average diameter of 82.01 nm.

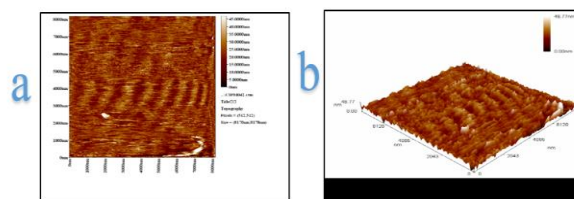


Fig 6. (a) AFM two-dimensional image for Sample CuO_n (b) AFM three-dimensional image for Sample CuO_n

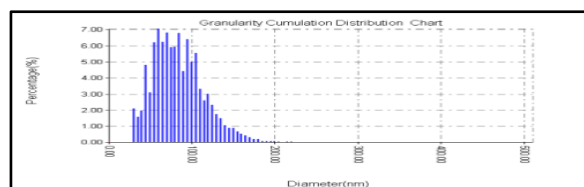


Fig 7. Granularity accumulation distribution for sample CuO_n.

3.1.4 FTIR Fourier-transform infrared spectroscopy

3.1.4.1 CuO_m Nanoparticles Synthesized by Microwave Enhancement

FTIR spectra of copper oxide micro is showed in fig 8, the wide amalgamation peak at approximately 375.665 mm⁻¹ was resulted by the adsorbed aqueous particles as the nano-crystalline resources have a elevated interfacial area, they absorb humidity. The peak at 298.185 mm⁻¹ is because of -C-H bond stretch assign to alkyl collection. The section between 270.0 and 375.0 mm⁻¹ is recognized as the OH-stretch section. The peaks at 168.206 is for the copper-Oxygen regular stretch. The various IR absorption peaks show the vibration mode copper oxide nanoparticles in range of 50 - 90 mm⁻¹. The little peak move in the vibration mode is linked with the matching alter in the face area of the set copper oxide nano-particles [8].

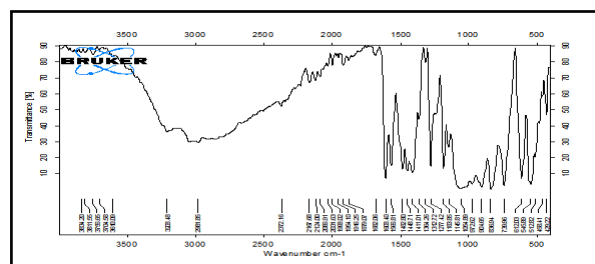


Fig 8. FTIR spectrum of CuO_m.

3.1.4.2 CuO Copper Oxide Nanoparticles

The FTIR spectra of copper oxide result are shown in Figure 9. We can see in this figure the wide absorption peaks, approximately 344.589 mm⁻¹ was resulted by the adsorbed aqueous particles as the nano-crystalline resources have an elevated

interfacial area, they absorb humidity. The peak at 292.221 mm⁻¹ is because of -C-H bond stretch assign to alkyl cluster. The section between 270 and 375 mm⁻¹ is recognized the OH-stretch section. The peaks at 163.277 is for Cu-O regular stretch. The two IR absorption peaks make known the vibration mode of copper oxide-NPs in range of 50 - 70 mm⁻¹. The peaks were showed at 53.333 mm⁻¹ and 58.441 mm⁻¹, correspondingly. The peak at 53.333 mm⁻¹ is because of stretching of copper-oxygen, which match up to the mode of B2u. The little peak move in the vibration mode is linked with the matching alter in the face area of the made copper oxide-nanoparticles. The peaks at 53.333 mm⁻¹ and 58.541 mm⁻¹ showed the configuration of the opper oxide-nanoparticles. The two peaks carry the attendance of mono-clinic stage. No other IR-active mode are indicated in range of 50- 70 mm⁻¹, which completely regulations out the continuation of Cu₂O. Peaks at 52.5 mm⁻¹ and 58.0 mm⁻¹ in FTIR spectra documented for copper oxide-nano-particles which close connected with our consequences. Consequently, the metal-oxygen frequencies showed for copper oxide-nanoparticles are in close accord with that of previous work literature principles [3].

3.2 Adsorption Process

3.2.1 Effect of contact time

The adsorption experimental runs were conceded out utilizing 0.05 L aqueous solution containing (50 to 125) ppm of heavy metals solution and (100 to 300) mg of adsorbent at ambient temperature with fixed pH value of 7, table 2 below shows the removal efficiency at equilibrium time for Cadmium and Figure7 shows the variation in the percentage removal cadmium with contact time, The removal of ions by CuO_m was a very rapid process where the percentage of removal begins to increase at the beginning of the experiment and up to the time of equilibrium 60 min, where stabilization the percentage of removal or begins to decrease, because there was more surface area of the adsorbent available for the metals' adsorption, and because the adsorption sites quickly ran out after the equilibrium time[9]. The same behavior for the different concentrations.

dose	CuO _m	CuO _n
0.1	%38	%0.43
0.15	%69	%4
0.2	%77	%6
0.25	%87	%6
0.3	%94	%1

Table 2. (a) Removal ratio at equilibrium time for 50 ppm of metal and PH 7 (b)Removal ratio at equilibrium time for metal and PH 7 on 0.25 g dose

Metal (ppm)	CuO _m	CuO _n
75	%63	%16
100	%57	%9
125	%51	%2

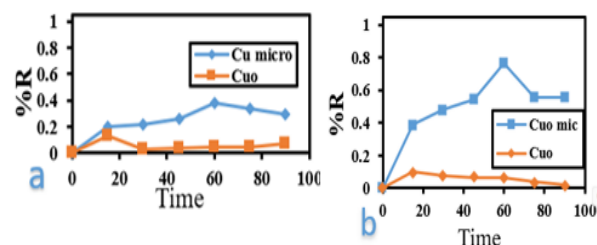


Fig 7. Percentage removal for 50 ppm Cd (II) and PH=7 (a). 0.1 g (b).0.3 g dose

3.2.2 Effect of pH

So as to show the effect of hydrogen function on the adsorption of the Cu Nano-composites experimental samples have been conceded out at preliminary concentration of 100 ppm and adsorbent concentration 0.25 g for sample in the pH range 2.0–12.0. Percentage removal of cadmium as a function of pH is shown in figure 8 Concentration of ion of hydrogen performs an active role on active pores and determines the surface charge of adsorbent in addition to the heavy metal removal throughout the adsorption process, the degree of ionization and speciation of the adsorbate, the rate of removal of heavy metals increases with increasing pH, solution of Cd (II) ions in synthetic wastewater is mainly controlled by pH of the solution. The optimal pH for Cd (II) removal was 7 was (57%), the exposed lower dosage in an sour medium is because of particle abrasion, incomplete protonation of useful group and the rivalry involving H⁺ and heavy metal ions for compulsory to the adsorption pores of the solid adsorbent. At pH higher than 7 Due to the production of hydroxides and the rapid rate of elimination due to sorption, both metals precipitated [2].

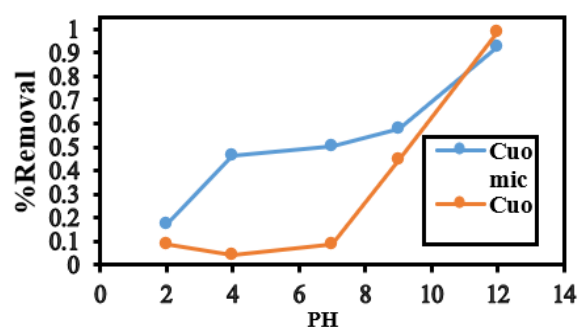


Fig 8. Percentage removal for Cd (II) at 100 ppm and equilibrium time and 0.25 g of dose.

3.2.3 Effect of adsorbent dose

The results investigating the effect of adsorbent dosage on Cd (II) ions removal with an initial concentrations 50 ppm and equilibrium time and pH 7 are shown in Figure 9 The metals ions adsorption is showed to raise as the quantity of adsorbent is improved slowly from 100 mg to 300 mg. The maximum adsorption effectiveness of cadmium on the adsorbents of catalyst have been exposed, the fig shows the likelihood to eliminate was 76% for CuO_m. The most adsorption is resulted at the adsorbent dosage of 300 mg where a additional

raise afterward, in the amount of the solid adsorbent up to 300 mg has negligible effect to the rate of adsorption. The data exposed that raising the weight of adsorbent will improve the adsorption of heavy metals since the number of metal vacant sites increase as well whether it is presented individually or with the other pollutants. Longer residence time supplies sufficient period for the sorption process to occur and therefore improve the metal ions dose from the aqueous solution on the metal compulsory pores of adsorbent [10].

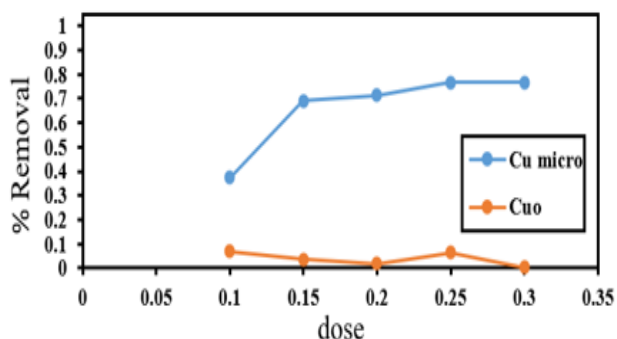


Fig 9. Percentage removal for Cd (II) at 50 ppm and equilibrium time

3.2.4 Effect of Adsorbate concentration

The effectiveness of the adsorption of metals has been tested as a function of the preliminary metal attentiveness. The concentration of heavy metals ion was in use between 50 to 125 mg/L, the hydrogen function of the solutions was fixed to 7 and concentration at 0.25g adsorbent dose, the experiments were conducted at ambient temperature, and the concentration of heavy metals was determined at equilibrium time, The percentage of heavy metals removed by copper nanocomposites depends on their initial concentration, is shown in Fig 10. The figure shows that the percentage removal for Cd (II) falls as the initial heavy metal concentration rises; it is most efficient at 50 ppm beginning concentration, after which the percentage removal decreases gradually to 48%. This reduce in adsorption occur with relative to the ions of the heavy metals attentiveness are explained in the low pouring force of mass transport or for a small active pores due to raise in concentration of metal [11].

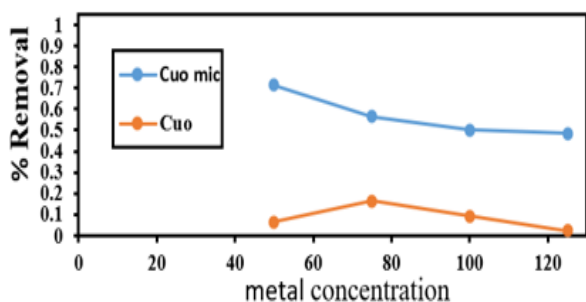


Fig 10. Percentage removal for Cd (II) at 0.25 g dose and equilibrium time and PH 7

Conclusions

Prepared copper Nanocomposites samples show a good agreement with the standard XRD pattern. And for adsorption experiments of CuO the efficiency of removal decreases as heavy metal concentration increase and the amount of adsorbents increase the removal increase as a result of the more available active site. The best pH solution was that of neutral with 7 since gave high removal compared to acidic and alkali. And for CuO was inefficient for all condition .

References

1. Lasheen MR, El-sherif IY, El-wakeel ST. Heavy metals removal from aqueous solution using magnetite Dowex 50WX4 resin nanocomposite. 2017;8(Vi):503–11.
2. Boudaoud A, Djedid M, Benalia M, Ad C, Bouzar N, Elmsellem H, et al. REMOVAL OF NICKEL (II) AND CADMIUM (II) IONS FROM WASTEWATER BY PALM FIBERS Mohamed 1 University , Faculty of Sciences , Department of Chemistry ,. 2017;18(4):391–406.
3. Luna IZ, Hilary LN, Chowdhury AMS, Gafur MA, Khan N, Khan RA. Preparation and Characterization of Copper Oxide Nanoparticles Synthesized via Chemical Precipitation Method. 2015;1–8.
4. Abd-Elkader OH, Deraz NM. Synthesis and characterization of new copper-based nanocomposite. International Journal of Electrochemical Science. 2013;8(6):8614–22.
5. Ali ISM. Preparation and Characterization of Copper Nanocomposite Catalysts and its Activity for Adsorption of Lead from Aqueous Solution Abstract: 2017;20(3):578–84.
6. Coman V, Robotin B, Ilea P. Nickel recovery/removal from industrial wastes: A review. Resources, Conservation and Recycling. 2013; 73:229–38.
7. Manuscript A. The Development of a Highly Photostable and Chemically Stable Zwitterionic Near-Infrared Dye for Imaging Applications. 2013;(207890).
8. Zhou Z, Lu C, Wu X, Zhang X. Cellulose nanocrystals as a novel support for CuO nanoparticles catalysts: Facile synthesis and their application to 4-nitrophenol reduction. RSC Advances. 2013;3(48):26066–73.
9. Petrus R, Warchol JK. Heavy metal removal by clinoptilolite. An equilibrium study in multi-component systems. Water Research. 2005;39(5):819–30.
10. Thakur LS, Parmar M. Synthetic Wastewater by Tea Waste Adsorbent. International Journal of Chemical and Physical Sciences. 2013;2(6):6–19.
11. Dermentzis K, Valsamidou E, Lazaridou A, Kokkinos NC, Ibtehal K, Shakir and Besma I. Husein. Journal of Engineering Science and Technology. 2011;4(2):188–92.